

Modeling of Readback Signal Generated by Scanning PCM Surfaces

Ilias Zaharias and Theodore Antonakopoulos
Department of Electrical and Computers Engineering
University of Patras
Patras, 26500, Greece
izacharias@ece.upatras.gr, antonako@upatras.gr

Abstract—Micro-electro-mechanical systems (MEMS) based on Scanning Probe Methods (SPM) are an emerging technology for sensor based applications and data storage. Atomic Force Microscope (AFM) techniques with conductive tips, using phase-change materials to record data as amorphous or crystalline marks, have been demonstrated experimentally. Storing data patterns on the Phase Change Medium (PCM) is achieved by the *write* process, which determines the final shape and size of the mark based on complex electrical, thermal and phase transition phenomena. The *read* process relies on measuring the electrical resistivity at different positions of the respective mark. In this paper, we present the model of the readback signal that is generated when a data pattern stored in a PCM surface is scanned with constant velocity. The presented two-dimensional model is based on Finite Element Method (FEM) analysis that has been used to simulate such a physical mechanism. The main objective of this work is to derive and analyze the basic waveform of the readback signal from an amorphous mark, for different geometric and physical configurations of the storage system.

Index Terms—Phase change medium, pulse modelling, read-back signal

I. INTRODUCTION

In recent years, there is an increased demand for micro-sensor applications and ultra-high density data storage systems based on nanotechnology. Micro-electro-mechanical systems (MEMS) are the most promising future technology that seems to deal well with such demanding applications. With MEMS devices it is possible to develop techniques to manipulate a sample material down to the nanometer scale. Techniques that use tips of a few nanometers for surface imaging and modifying nano-structures have been widely investigated [1]. MEMS storage systems based on Atomic Force Microscope (AFM) make use of nanometer scale sharp tips for sensing the structure (topology) or physical properties of a material. The most well-known scanning-probe-based approach for data storage is that of the IBM “Millipede” system, where a thermo-mechanical probe is used to write, read and erase indentations in a polymer film [2], [3].

Recently, phase-change materials that employ chalcogenide alloys, such as *GeSbTe* or *AgInSbTe*, have been used for optical storage systems and PCRAM device applications [4], [5], [6], [7]. This technology relies on the reversible transition property of phase change materials between amorphous and (poly)crystalline state via joule heating. In a scanning-probe Phase Change Medium (PCM) system, there is a conductive

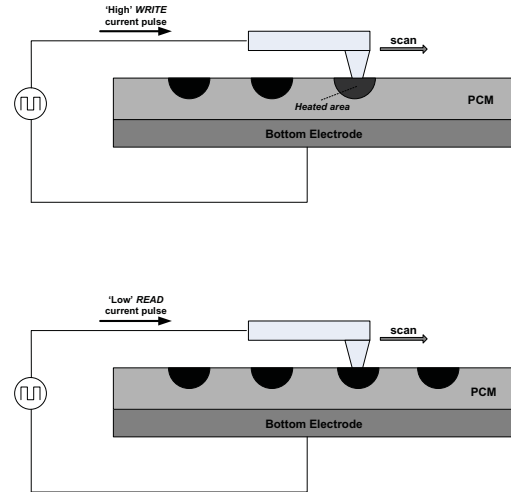


Fig. 1. A scanning-probe system based on phase-change materials, showing the write (up) and read (down) operations.

probe/tip in contact with the medium, so that electric current can flow from the probe through PCM ([8], [9], [10]). Information is stored across a track as sequences of “marks” and “no marks” written in a nanometer-thick phase change material. In storage applications, the presence or absence of an amorphous/crystalline mark corresponds to the logical value “1” or “0”, respectively. In addition to storage systems, pre-stored PCM data patterns can be used in sensors to measure various physical quantities. For example, PCM surfaces with two dimensional data patterns can be used in accelerometers to estimate/measure the speed and acceleration applied to a MEMS system.

Section II presents the basics of PCM technology and surface imaging using scanning probes, while Section III analyzes the Finite Element Method (FEM) model used for studying the PCM mark. The PCM read process is highlighted in Section IV and various simulation results are presented and analyzed. Finally, Section V presents the PCM pulse model that fits the experimental results and its analytic expression.

II. PCM SCANNING-PROBE SYSTEM

A simplified scanning-probe system architecture is shown in Fig.1. That system is comprised of a two-layer structure:

The uppermost layer, which is the PCM medium and the highly conductive underlayer that forms the bottom electrode. Write/Read operations depend on mechanical scanning with a probe moving at constant velocity relative to the PCM medium. During *write* (see Fig.1) the probe moves relative to the medium and an electrical voltage pulse is applied to the tip with respect to the bottom electrode at regular time instants and proper displacements. That process causes a current flow that heats locally the PCM, beneath the tip-medium contact area. If the pulse amplitude and duration are sufficient, the PCM will reach the required temperature and the phase transition process will be initiated. The physical mechanisms that take place during the writing operation as mentioned so far, involve electrical, thermal and phase transition processes. The electrothermal process and the physical characteristics of the probes and the medium define the current density that leads to temperature variations and the formation of marks.

Writing an amorphous mark in a crystalline material, requires heating the PCM above melting temperature ($616\text{ }^{\circ}\text{C}$ for $\text{Ge}_2\text{Sb}_2\text{Te}_5$) by applying a short and intense electrical pulse. A subsequent rapid quenching of the melted region, below its glass transition temperature, with rates of the order of a few tens of K/ns, allows the material to solidify in the amorphous state [11], [12]. It should be mentioned that the mark size is substantially smaller than the PCM layer thickness and it has a semi-spherical shape localized to the upper portion of the PCM layer, near the tip-medium contact area. The writing process is performed only once at the beginning of the lifetime of such a device, while the energy efficient read process is performed during surface imaging.

The process of *read* is based on a similar concept. As demonstrated in Fig.1, during *read* the tip scans the surface over the written 'marks' across the track and a voltage pulse is applied between the tip and the bottom electrode, resulting in a current flow that provides the read-back signal. The applied voltage is lower than that in the writing process, so that any heating is negligible and no phase transition is activated. The *read* process relies on the vastly difference between electrical conductivities of the amorphous and crystalline phases of the PCM layer. Hence, the detection of the underlying mark is done by sensing the equivalent resistance of the probe-medium system. Depending of the physical characteristics of that system and the speed of movement, an number of read pulses is applied per 'mark' for reconstructing accurately the readback signal.

III. THE MODEL OF THE PCM MARK

As mentioned above, the write/read processes couple electrical, thermal and phase change transition physical phenomena, as well as moving parts (probe). To investigate these phenomena in detail and to explore the performance of such a system, we have developed a comprehensive simulation model, which enables a systematic numerical analysis and description of the system's operations. In order to create a complete and accurate model we used the Comsol Multiphysics computational tool

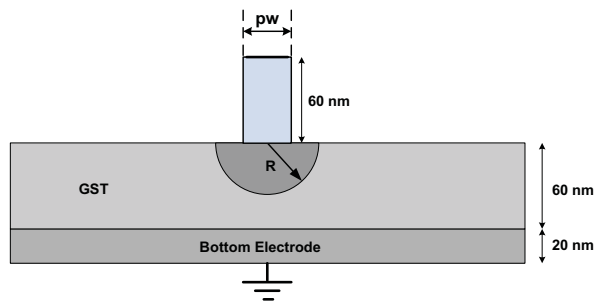


Fig. 2. Geometry of the read-back model.

[13], that is based on finite element numerical methods, in conjunction with the Mathworks Matlab environment [14].

A. Geometry of the PCM Model

The developed model, shown in Fig.2, is a two-dimensional structure and consists of three main parts. The probe-tip element and two-layered substrates. The element at the top of the structure is designed on purpose to be relatively high enough, to correspond with both probe and tip as a whole. The tip-width is not associated with the physical sharpness of the tip but with the electrical tip-medium contact area. In a real system, it is possible to have tips with small electrical contact interface but large physical contact radius. It is important to note that in electrical probe recording, the written bit size and the readback signal resolution are primarily determined by the tip-medium electrical contact area. In sensor applications different probes may be used for read and write, since wider probes may result to larger PCM marks.

The two-layer rectangular structure is comprised of the $\text{Ge}_2\text{Sb}_2\text{Te}_5$ material (referred to elsewhere in this paper as GST) which is 60 nm thick and the highly conductive ($\sigma = 10^6\text{ S/m}$) bottom electrode (underlayer). The dimensions used in this model were selected so that there is enough space to form a semi-spherical PCM 'mark', while the height of the bottom electrode does not affect the whole model. Notice that the width of the substrate is considered to be large enough (500 nm) compared with the tip-width, as well as the probe-scanning area (maximum $\pm 100\text{ nm}$) assumed for the simulations. The basic parameters of this model are pw , the diameter of the top electrode and R , the radius of the PCM 'mark'. We always consider that $pw < R$, otherwise the PCM pulse has always low resistance with low variability.

The model incorporates all the physical processes referred previously by solving the necessary time-dependent equations. The writing procedure which is too complicated, including electrothermal and phase transition processes, is beyond the scope of this paper and it will not be discussed here. Instead, we will focus our analysis on the *read* process and particularly the detection of a single written amorphous mark inside a crystalline phase-change material.

B. The Electrical Model and its Parameters

The *read* operation is purely electrical and mainly depends on material properties and the physical parameters of that

TABLE I
ELECTRICAL CONDUCTIVITIES OF ELEMENTS

Element	σ (S/m)
Probe/tip	10^6
$GST_{amor.}$	3
$GST_{cryst.}$	3000
Bottom electrode	10^6

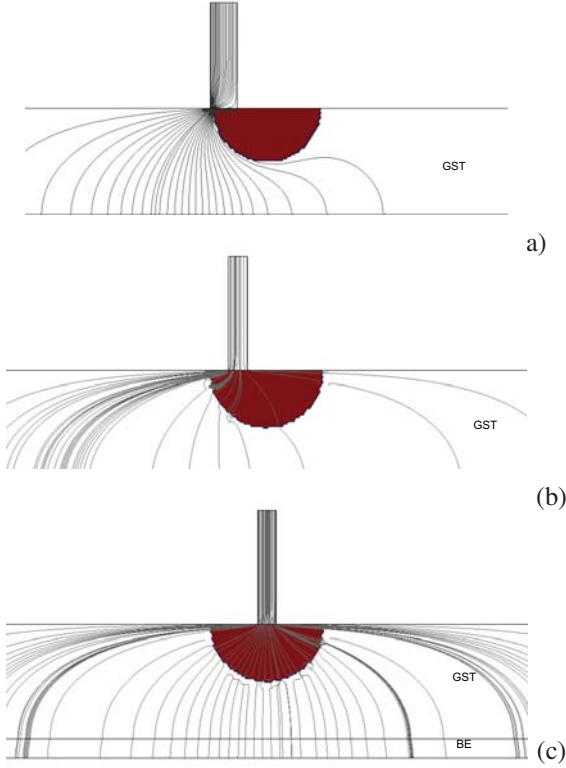


Fig. 3. Snapshots of the simulation scanning showing the current density (streamline) in different locations of the tip relative to the PCM mark: (a) just before the tip entirely enters above the amorphous region, (b) as the tip is located between the center and the boundary of the mark, and (c) at the center of the mark.

system. The electrical solution of the model is derived by solving the Laplace equation of the electric field theory

$$\nabla \cdot [\sigma(x, y) \nabla V(x, y, t)] = 0 \quad (1)$$

where σ is the electrical conductivity and V is the electric potential. Solving this time-dependent equation we can determine the potential V , electric field \vec{E} and current density \vec{J} throughout the system's structure. The Laplace equation requires electrical conductivities of the materials that assumed for this model, which were derived from other published works ([11], [12]) and are given in Table I.

IV. THE READ OPERATION

During *read*, a set of equally spaced voltage pulses is applied to the upper bound of the probe-tip, while the lower bound of the bottom electrode is maintained at ground potential. Insulation conditions are assigned to all other exterior

boundaries and continuity to the interior boundaries. Each voltage pulse that is applied to the system, has square waveform characteristics, relatively short duration (20 nsec) and low amplitude (0.2 V) to avoid re-crystallization via heating. To simulate the scanning mechanism, it was considered that the tip was stationary above the GST medium for each voltage pulse duration and moving forward with a space increment of 1 nm for the next loop. Each applied voltage pulse (at every tip position) results to a current flow throughout the tip-medium structure. In Fig.3 various snapshots of the current density are shown for different locations of the tip relative to the center of the PCM mark. As it can be seen from this figure, there is a highly conductive path (crystalline region) just before the tip entirely enters above the amorphous region, and in this case the current can flow through. In that state, the equivalent resistance is still low. When the tip is over the amorphous region, the current density drops radically, resulting to a high resistance state, even when the tip is not in the center of the mark. The distribution of the current relative to the position of the tip explains the pulse shape presented in Fig. 4(a).

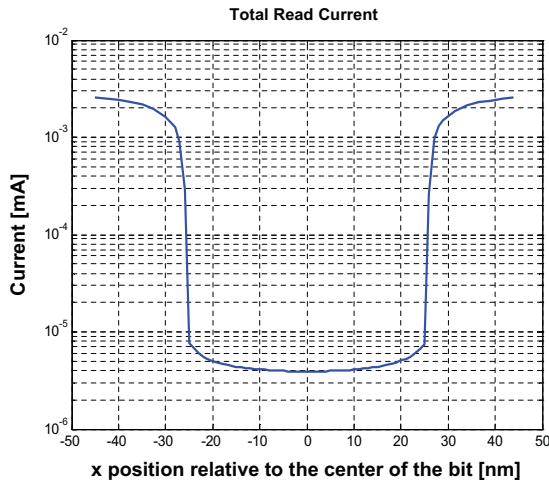
The ratio of the applied voltage amplitude V_p to the total current I , equals to the equivalent resistance of the system. Therefore, we can extract a function of the equivalent resistance that depends on position coordinate x and can be expressed as $R_{es}(x)$. This function, as it is shown in Fig. 4(b), has the form of a pulse. The main objective of this study, is to extract the typical readback pulse, for various geometric configurations. In particular, we study how the basic characteristics of the readback signal vary with respect to the physical characteristics of the simulated system, i.e. size of the written bit and the tip-width. For this reason, it was defined the parameter \mathbf{a} , which corresponds to the ratio pw/R , where $\mathbf{a} < 1$.

A. Simulation Results

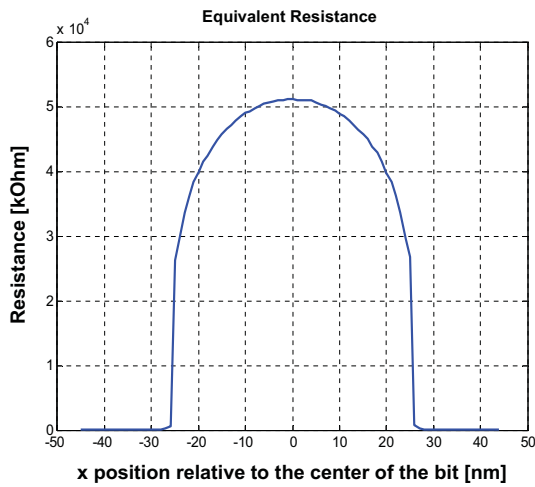
In this section, we present and analyze the simulation results for two different physical parameters, for the same chalcogenide medium. In particular, simulations have been executed for mark sizes of radius 20, 30 and 40 nm. For each of these cases, the amorphous mark was scanned for a wide range of tip-width, i.e different values of parameter \mathbf{a} .

Fig.4 (a) illustrates a typical form of the readback current pulse (in logarithmic scale) and Fig.4 (b) the equivalent resistance, for a mark size of radius $R=30\text{nm}$ and for $pw=6\text{nm}$. Notice that the resistance pulse can be divided into two states: the state that exhibits low resistance, when the tip is above the crystalline area and the high resistance state (around bit center), when the amorphous area is scanned. Moreover, the transition from low to high resistance state and vice versa becomes almost instantly, within a small space range, less than 1 nm. This is because there is a narrow region where the tip-medium electrical contact area is partially highly conductive and partially low conductive.

In these simulations, it was considered that an isolated amorphous mark has been written in the middle of the GST layer with a semi-spherical shape and for various radius values.



(a)

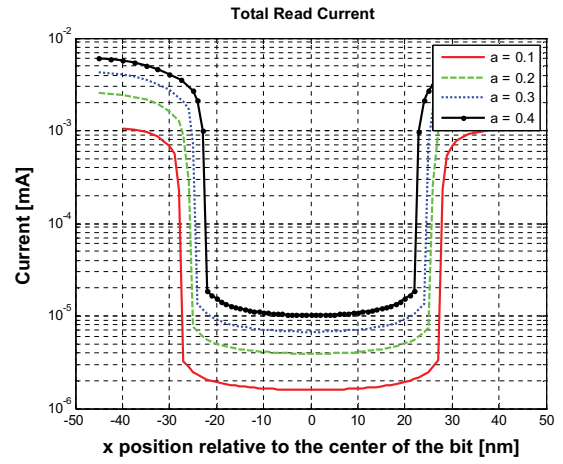


(b)

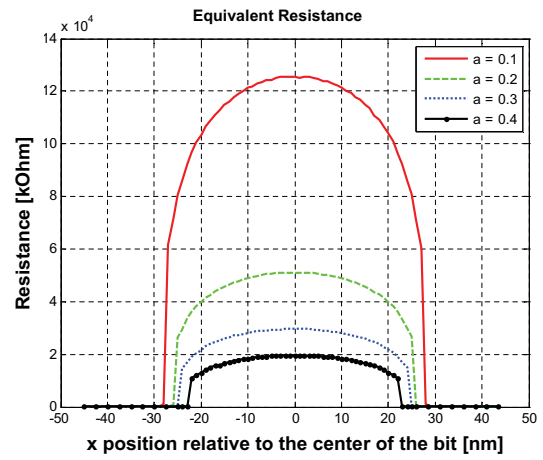
Fig. 4. (a) Readback current pulse (logarithmic scale) (b) Equivalent resistance for an amorphous mark with $R=30\text{nm}$.

The radius R of amorphous region and the tip-width pw , as illustrated in Fig.2 are the basic input geometric parameters.

Fig.5 illustrates the total current pulse and the equivalent resistance pulse for an amorphous mark of radius 30 nm and for four different values of parameter a (0.1-0.4). Note that in all cases, the pulses have a similar form and they mainly differ in *amplitude* and *width*. The amplitude of the resistance pulse decreases as the a parameter increases. The reason is that the electrical contact area becomes wider for larger values of a (as for pw) and more current can flow from the tip inside the GST for a constant voltage amplitude. Furthermore, the pulse *width* shortens for larger values of a . This is due to the fact that the tip-medium electrical contact area needs more distance to cover till completely entering above the amorphous region. Fig.6 shows the total current and resistance readback pulses for 3 different amorphous sizes of radius 20, 30 and 40 nm and for the same tip-width (6 nm). It should be mentioned that the pulse shape remains the same for all cases, as expected,



(a)



(b)

Fig. 5. (a) Readback current pulse (logarithmic scale) (b) Equivalent resistance pulse for 4 values of parameter a and for an amorphous mark with $R=30\text{nm}$.

and they differ in amplitude and width.

V. PULSE MODEL

As it was shown in Figs. 5 and 6, the form of the readback pulse exhibits the same basic characteristics which are independent of the mark size (radius) and the tip-medium contact area. From now on, we will concentrate our analysis to the equivalent resistance pulse of the readback signal. In Fig.7 a typical resistance pulse is depicted, which is derived by reading of a single 'mark'. As parameters we use the maximum amplitude R_{max} (observed at the center of the pulse), the pulse *width* and the quantity A_o . The pulse width is defined by the transition points from low to high resistance state and vice versa, while the quantity A_o corresponds to the magnitude of the transition gap.

We now investigate how these parameters depend on the geometric features of the system and particularly on parameter a , the ratio pw/R . The objective is to define an approximate but accurate formula that represents the readback pulse.

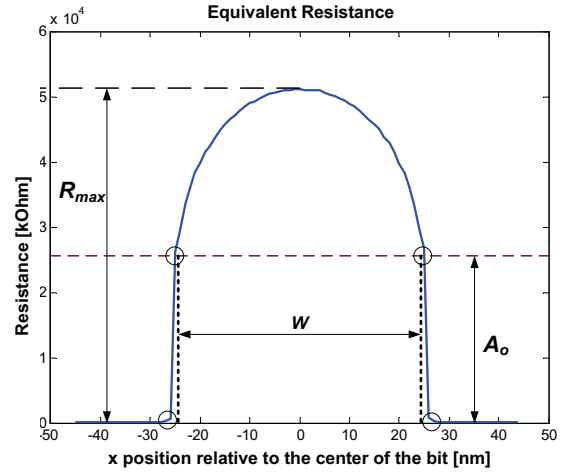
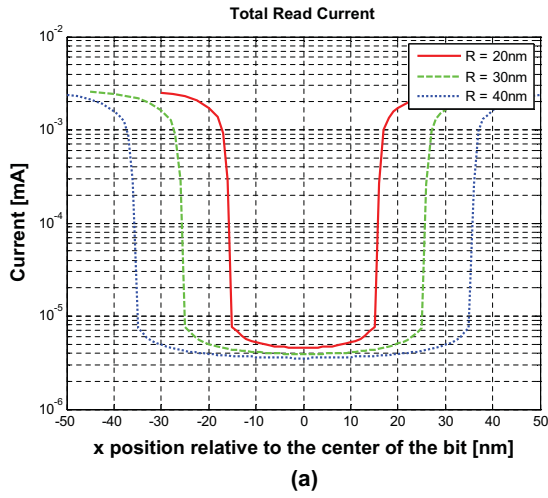


Fig. 7. Typical shape of the equivalent resistance pulse.

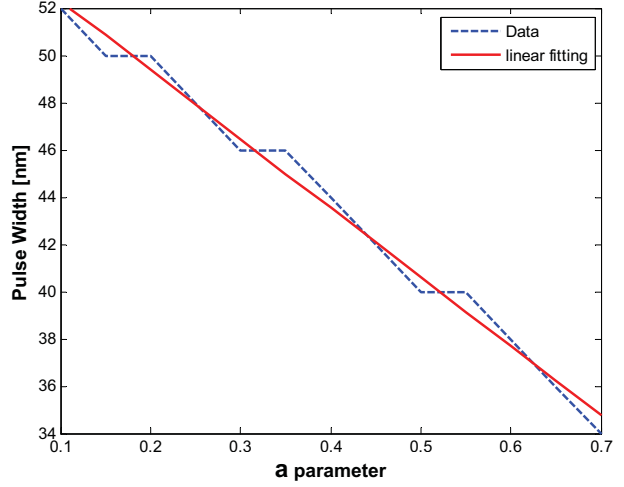
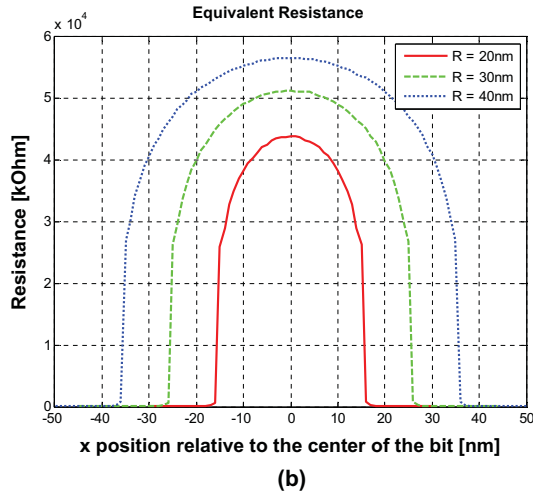


Fig. 6. (a) Readback current pulse (logarithmic scale) (b) Equivalent resistance for 3 amorphous mark sizes (radius).

Fig. 8. Pulse width of the readback signal with respect to parameter a for an amorphous mark radius $R=30\text{nm}$.

The parameters R_{maxN} and A_{oN} are independent of the size (radius) of the written amorphous mark and they mainly depend on the parameter a . The same holds also for the pulse width W .

The third parameter that is examined here, is the pulse width W . Fig.8 illustrates the dependence of parameter a on the pulse width as extracted from the simulation results (dashed line). The figure also show an approximation of the data with a linear function (red line).

The part of the readback pulse that is confined by $A_o \leq R_{es(x)} \leq R_{max}$ and $-\frac{W}{2} \leq x \leq \frac{W}{2}$ needs further investigation. Fig.9 illustrates the function $G(x)$ corresponding to this part of the pulse, defined as $G(x) = R_{es(x)} - A_o$, for $-\frac{W}{2} \leq x \leq \frac{W}{2}$ and an approximation of this function with a 4th degree polynomial.

Considering that $P(x)$ is the function corresponding to the readback resistance pulse, it can then be described as

$$P(x) = \begin{cases} G(x) + A_o & \|x\| \leq \frac{W}{2} \\ a_1x + b_1 & \text{for } -\frac{W}{2} - l \leq x < -\frac{W}{2} \\ a_2x + b_2 & \text{for } \frac{W}{2} < x \leq \frac{W}{2} + l \\ e & \text{elsewhere} \end{cases} \quad (2)$$

where x is the position coordinate in nm , W the pulse width and a_1, a_2, a_3 and a_4 coefficients. Constant e has a small positive value ($e > 0$) corresponding to the low-resistance level. The parameter l is equal to the transition interval.

VI. CONCLUSIONS

In order to exploit the readback signal generated when PCM surfaces are scanned, the respective pulse model is needed in order to design the signal processing algorithms for extracting a specific characteristic. For example, combining data patterns of specific statistical properties with the signal generated when such a pattern is sensed with variable speed may result in accurate estimation of motion characteristics in MEMS-based

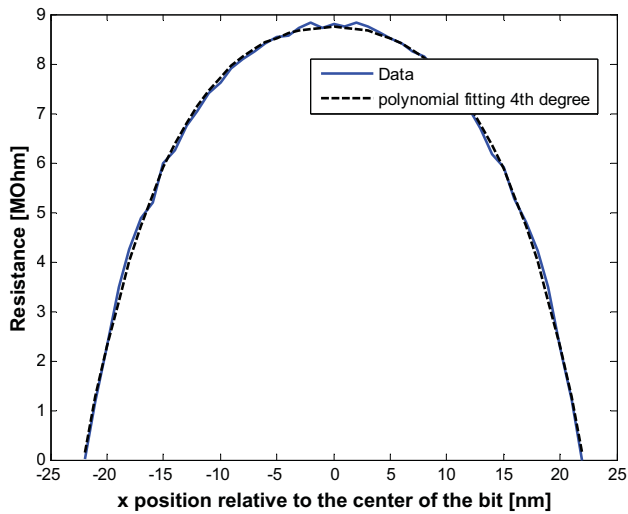


Fig. 9. Function $G(x)$ for an amorphous mark with $R=30\text{nm}$.

sensors, if the pulse model is available for constant speed scanning.

In this work we studied the resistive pulse that corresponds to such a scanning process and as the simulation results show, the basic shape of the readback signal is independent of the geometric configuration of the system, for semi-spherical amorphous ‘marks’, while specific pulse parameters can be associated with system’s physical properties. The readback pulse of such a system can be divided into three main zones with respect to the resistance levels and the transition points. There are two main resistance levels: the low-resistance level (almost constant) and the high resistance level (described by the above mentioned function $G(x)$) corresponding to crystalline and amorphous scanning areas respectively, while the transition from low to high resistance and vice versa becomes almost instantly.

REFERENCES

- [1] Ampere A. Tseng, Ed., *Nanofabrication: Fundamentals and Applications*. World Scientific, 2008.
- [2] P. Vettiger, G. Cross, U. Drechsler, U. Durig, B. Gotsmann, W. Haberle, M.A. Lantz, H.E. Rothuizen, R. Stutz, and G.K. Binning , “The millipede-nanotechnology entering data storage,” *IEEE Transactions on Nanotechnology*, vol. 1, no. 1, pp. 39–55, 2002.
- [3] E. Eleftheriou, Th. Antonakopoulos, G. K. Binnig, G. Cherubini, M. Despont, A. Dholakia, U. Durig, M. A. Lantz, H. Pozidis, H. E. Rothuizen and P. Vettiger, “Millipede - a mems-based scanning-probe data-storage system,” *IEEE Transactions on Magnetics*, vol. 39, no. 2, pp. 938–945, 2003.
- [4] A. Pirovano, A. Lacaita, F. Pellizzer, S. Kostylev, A. Benvenuti, and R. Bez, “Low-field amorphous state resistance and threshold voltage drift in chalcogenide materials,” *IEEE Trans. Electron Devices*, vol. 51, no. 5, pp. 714–719, May 2004.
- [5] H. Satoh, K. Sugawara, and K. Tanaka, “Nanoscale phase changes in crystalline $\text{ge}_2\text{sb}_2\text{te}_5$ films using scanning probe microscopes,” *J. Appl. Phys.*, vol. 99, pp. 024 306–1–024 306–7, 2006.
- [6] T. Gotoh, K. Sugawara, and K. Tanaka, “Minimal phase-change marks produced in amorphous $\text{ge}_2\text{sb}_2\text{te}_5$ films,” *Jpn. J. Appl. Phys.*, vol. 43, no. 6B, pp. L818–L821, 2004.
- [7] M. Wuttig, N. Yamada, “Phase-change materials for rewritable data storage,” *Nature Materials*, vol. 6, pp. 824–832, 2007.
- [8] C.D. Wright, M. Armand, and Mustafa M. Aziz, “Terabit-per-square-inch data storage using phase-change media and scanning electrical nanoprobes,” *IEEE Transactions on Nanotechnology*, vol. 5, no. 1, Jan. 2006.
- [9] C.D. Wright, Wang L., P. Shah, Mustafa M. Aziz, E. Varesi, R. Bez, M. Moroni, and F. Cazzaniga , “The design of rewritable ultrahigh density scanning-probe phase-change memories,” *IEEE Transactions on Nanotechnology*, vol. 10, no. 4, 2011.
- [10] Mustafa M. Aziz and C.D. Wright, “An analytical model for nanoscale electrothermal probe recording on phase-change media,” *J. Appl. Phys.*, vol. 99, pp. 034 301–1–034 301–12, 2006.
- [11] D.H. Kim, F. Merget, M. Forst, and H. Kurz, “Three-dimensional simulation model of switching dynamics in phase change random access cells,” *J. Appl. Phys.*, vol. 101, pp. 064 512–1–064 512–12, 2007.
- [12] J. Reinenberg, E. Pop, A. Gibby, S. Wong, K. Goodson, “Multiphysics modeling and impact of thermal boundary resistance in phase change memory devices,” in *ITHERM '06. The Tenth Intersociety Conference on*, 2006, pp. 106–113.
- [13] Comsol Multiphysics Website. [Online]. Available: <http://www.comsol.com/>
- [14] The MathWorks Website. [Online]. Available: <http://www.mathworks.com/>